

Comparative Bending Dynamics in DNA with and without A-tracts

Alexey K. Mazur and Dimitri E. Kamashev
Laboratoire de Biochimie Théorique, CNRS UPR9080
Institut de Biologie Physico-Chimique
13, rue Pierre et Marie Curie, Paris, 75005, France.
FAX: +33[0]1.58.41.50.26. Email: alexey@ibpc.fr

The macroscopic curvature of double helical DNA induced by regularly repeated adenine tracts is well-known but still puzzling. Its physical origin remains controversial even though it is perhaps the best-documented sequence modulation of DNA structure. We report here the results of comparative theoretical and experimental studies of bending dynamics in 35-mer DNA fragments. This length appears large enough for the curvature to be distinguished by gel electrophoresis. Two DNA fragments, with identical base pair composition, but different sequences are compared. In the first one, a single A-tract motif was four times repeated in phase with the helical screw whereas the second sequence was "random". Both calculations and experiments indicate that the A-tract DNA is distinguished by the large static curvature and characteristic bending dynamics, suggesting that the computed effect corresponds to the experimental phenomenon. The results poorly agree with earlier views that attributed a decisive role in DNA bending to sequence specific base pair stacking or binding of solvent counterions, but lend additional support to the hypothesis of a compressed frustrated state of the backbone as the principal physical cause of the static curvature. We discuss the possible ways of experimental verification of this hypothesis.

INTRODUCTION

It is generally accepted that the base pair sequence can affect the overall form of the DNA double helix. Intrinsic DNA bending is the simplest such effect. Natural static curvature was discovered nearly twenty years ago in DNA containing regular repeats of A_nT_m , with $n + m > 3$, called A-tracts^{1,2,3}. Since then this intriguing phenomenon has been actively studied, with several profound reviews of the results published in different years^{4,5,6,7,8,9}. It is known that the curvature is directed towards the minor grooves of A-tracts and/or the major grooves of the junction zones between them, and that its magnitude is around 18° per A-tract. However, the exact sites and the character of local bends remain a matter of debate as well as their mechanism and physical origin.

Already the pioneering conformational calculations of the seventies showed that the DNA double helix exhibits significant bendability which is anisotropic and sequence dependent^{10,11}. Based upon these views the wedge model offered the very first explanation of bending induced by A-tracts by postulating that stacking in ApA steps is intrinsically non-parallel¹². Modified versions of this the-

ory accounted for a substantial part of available experimental data, with good scores of curvature prediction from sets of fitted wedge angles^{13,14,15}. At the same time, clear experimental counter-examples exist where bending could not result from simple accumulation of wedges^{16,17}. The junction model^{18,2} better than other theories explained experimental data on gel retardation of curved DNA. It originated from an idea that a bend should occur when two different DNA forms are stacked¹⁹. If poly-dA double helix had a special B' form as suggested by some data²⁰ the helical axis should be kinked when an A-tract is interrupted by a random sequence. In turn, the X-ray data are best interpreted with an alternative theory that postulates that bending is intrinsic in most DNA sequences except A-tracts which are straight^{21,22,23}. Another interesting model attracted attention in the recent years, namely, bending by electrostatic forces that result from neutralization of phosphates by solvent cations trapped in the minor grooves of A-tracts²⁴. This problem is of general importance because the accumulated large volume of apparently paradoxical observations suggests that some essential features are still unknown that may be essential for the fine structure and the biological function of the DNA molecule.

One of us has recently proposed a new hypothesis of the physical origin of intrinsic bends in double helical DNA²⁵. According to it, the sugar-phosphate backbone in physiological conditions is slightly compressed, that is the equilibrium specific length of the corresponding free polymer in the same solvent is larger than that in the canonical B-form. Therefore, the backbone "pushes" stacked base pairs, forcing them to increase the helical twist and rise while the stacking interactions oppose this. As a result, the backbone increases its length by deviating from its regular spiral trace and wanders along the helical surface causing quasi-sinusoidal modulations of DNA grooves. Concomitant base stacking perturbations result in macroscopic static curvature when certain properties of base pairs alternate along the sequence in phase with the helical screw.

Drew and Travers (1984, 1985) apparently were the first to notice that narrowing of both DNA grooves at the inner edge of a bend is a necessary and sufficient condition of bending, and that an unusual local groove width should be accompanied by structural perturbations beyond this region. They, and later Burkhoff and Tullius (1987), considered the preference of narrow and wide minor groove profiles by certain sequences as the pos-

sible original cause of this effect. Sproun et al (1999) proposed a similar idea within the context of the junction model. In a certain sense, the compressed backbone theory continued the same line of thinking. Unlike other models, it naturally explains well-known environmental effect upon the A-tract curvature, notably, its reduction with temperature^{26,27,28} and addition of dehydrating agents^{29,30,31} (see discussion in Mazur (2000)). This theory certainly needs further examination and critical comparison with other models in both calculations and experiments.

Conformational modeling earlier helped to shed light upon many aspects of the above problems. Construction of spatial DNA traces from local wedge parameters combined with Monte Carlo simulations of loop closure was applied to check different hypotheses and to estimate local bending angles from experimental data^{18,32}. Energy calculations revealed that bending may be easier at some dinucleotide steps and in certain specific directions^{11,33}, with experimental sequence effects reproduced in some remarkable examples³⁴. DNA was shown to have local energy minima in bent conformations corresponding to the junction model^{35,36}. All atom Monte Carlo calculations showed that narrowing of the A-tract minor groove with a few NMR-derived restraints may be sufficient to provoke the curvature³⁷.

The simplest set-up for modeling DNA bending is to take a straight symmetrical double helix and let it bend spontaneously with no extra forces applied, that is due to generic atom-atom interactions. This “naive” approach has recently become possible owing to the progress in methodology of molecular dynamics (MD) calculations of nucleic acids³⁸, which was demonstrated by successful simulations of several curved and straight DNA fragments in realistic environment including explicit water and counterions^{39,40}. The character of bending qualitatively agreed with the theories outlined above so that none of them could be preferred. Thorough discriminative testing would require more extensive sampling of bending events, which should become possible in future. Detailed structures of short A-tract fragments have also been studied by MD^{41,42}.

The major obstacle in free MD simulations of intrinsic curvature is the limited capacity of sampling of bending events. The physical time of transition between straight and bent conformations may be too long for a statistically significant number of such events to be accumulated in simulations. Moreover, experimental effects may not appear during infinitely long MD because models are never perfect. To circumvent these difficulties, we employed a different strategy. We first looked for, and found a short A-tract motif that could reproducibly induce stable bends in DNA during a few nanoseconds of MD with a simplified model of B-DNA. We used this motif to construct longer double helices with intrinsic curvature *in silico* and we could increase the length of DNA fragments in calculations to 35 bp, which makes possible a direct comparison with experiments *in vitro*.

The two 35-mer DNA fragments we study here have identical base pair composition and differ only by their sequences. The first fragment is the designed A-tract repeat while the other sequence is “random”. All MD trajectories start from canonical straight A- and B-DNA conformations. For the A-tract DNA fragment they converged to a single statically bent state with planar curvature towards the narrowed minor grooves at 3’ ends of A-tracts. The magnitude of bending is close to the experimental estimates. The random fragment was not straight as well, but its curvature was much less significant and less planar. In gel migration assays the two molecules produce well-resolved distinct bands, with the A-tract sequence demonstrating a reduced mobility characteristic of curved DNA. These results suggest that the intrinsic DNA curvature reproduced in calculations corresponds to the experimental phenomenon. The bending dynamics qualitatively agrees with the compressed backbone theory, but it cannot be accounted for by other models.

MATERIALS AND METHODS

Calculations

Molecular dynamics simulations have been performed by the internal coordinate method (ICMD)^{43,44} including special technique for flexible sugar rings⁴⁵, with AMBER94^{46,47} force field and TIP3P water⁴⁸. All calculations were carried out without cut-offs and boundary conditions. The time step was 10 fsec. The so-called minimal model of B-DNA was used^{49,50}. It includes only a partial hydration shell and treats counterion and long range solvation effects implicitly. Advantages as well as limitations of this approach have been reviewed elsewhere³⁸. The model has no other bias towards bent or non-bent conformations except the base pair sequence.

The starting fiber A- and B-DNA models were constructed from the published atom coordinates⁵¹. The hydration protocols were same as before,²⁵ with an identical number of explicit water molecules in A- and B-DNA starts. Programs Curves,⁵² XmMol,⁵³ and Mathematica by Wolfram Research Inc. were employed for graphics and data analysis.

The two 35pb DNA fragments are referred to below as At and nAt, for the A-tract repeat and the non-A-tract DNA, respectively. For both fragments two long MD trajectories were computed starting from either A- or B-canonical DNA forms. These four trajectories are referred to as At-A, At-B, nAt-A, and nAt-B, respectively, where the last character indicates the starting state. All trajectories were continued to 20 ns except At-B which was stopped at about 12 ns because it had clearly converged long before.

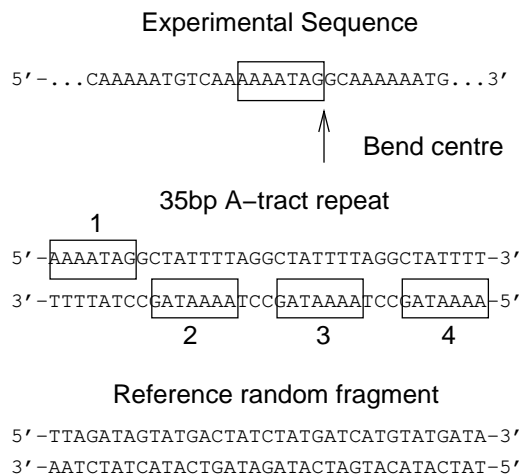


FIG. 1. Construction of 35 bp double stranded DNA fragments. The top sequence with the boxed heptamer motif AAAAATAG is taken from the trypanosome kinetoplast DNA². The A-tracts are numbered and their centers are separated by approximately 10 bp. The reference random fragment has the same base pair content as the 35-mer repeat, but its sequence has been manually re-shuffled to exclude any A-tract motives.

Oligonucleotides and construction of 5'-labeled DNA probes

The sequences of the 35 nt-long synthetic oligonucleotides used here are shown in Fig. 1. The double stranded DNAs were obtained by annealing of the two complementary oligonucleotides, one of them labeled with T4 polynucleotide kinase and [³²P]-ATP. The annealing was carried out by incubating the oligonucleotides (300 nM) for 3 min at 80°C in 20 mM Tris-HCl (pH 8.0), 400 mM NaCl, 0.2 mM EDTA and then allowing them to cool slowly.

Gel mobility assays

Mobility of the DNA fragments was analyzed in 16% gels (acrylamide to bis-acrylamide, 29:1) buffered with 90 mM Tris-borate, 1 mM EDTA, pH 8.6. Gels were pre-run under constant power until stabilization of current. End-labeled DNA in a buffer containing 20 mM Tris-HCl, 50 mM NaCl, 7% glycerol, pH 8.0 and bromophenol-blue was loaded onto the gel. The electrophoresis was performed under constant power and constant temperature of 8°C. The dried gels were exposed to storage phosphor screens and visualized on a 400S PhosphorImager (Molecular Dynamics).

RESULTS AND DISCUSSION

Construction of DNA Fragments

Figure 1 explains how the two DNA fragments used in our study have been constructed. The A-tract motif AAAAATAG originally attracted our attention in MD simulations of the natural DNA shown in Fig. 1⁵⁴, which is the first curved DNA locus studied *in vitro*². The 35 bp A-tract fragment was constructed by repeating this motif four times and it had to be inverted to make the two DNA termini symmetrical. Such inversion should not affect bending,⁵⁵ but is essential for simulations because the 3'- and 5'-end A-tracts may represent qualitatively different boundaries. In repeated simulations with this and similar A-tract fragments, the static curvature emerged spontaneously and it became more evident as the chain length increased²⁵. To obtain a reference non-A-tract DNA, we have re-shuffled manually base pairs of the A-tract repeat. We preferred this randomized sequence to commonly used GC-rich straight fragments in order to keep the base pair content identical and reduce the noise that could cause small variations in gel mobility and hide the subtle differences we were going to detect.

Spontaneous Development of Curvature in Simulations

All four trajectories exhibited stable dynamics with DNA structures close to the B form. Table I shows parameters of the final 1ns-average conformations. They all have remarkably similar helicoidals corresponding to a typical B-DNA. For example, the average helical twist estimated from the best-fit B-DNA experimental values⁵⁶ gives $34.0 \pm 0.2^\circ$ and $33.8 \pm 0.2^\circ$ for the A-tract fragment and the randomized sequence, respectively. At the same time, the rms deviations from the canonical structures vary more significantly.

As shown in Fig. 2, during the first few nanoseconds, the rmsd from the canonical B-DNA quickly leveled at around 4 Å in all four trajectories. For the A-DNA start this corresponds to a rapid transition to B-form with reduction of rmsd from the initial 10.7 Å. The subsequent dynamics is remarkably different for the At and nAt trajectories. In At-A and At-B, after some delay, the rmsd value drastically increased and stabilized at a higher level of around 6 Å. The traces of the bend angle and the axis shortening indicate that this was a transition to a significantly larger curvature. In contrast, for nAt trajectories, Fig. 2 exhibits only fluctuations at roughly the same level as in At-A and At-B before the transition.

TABLE I. Some structural parameters of standard and computed DNA conformations. The helicoidals are the sequence averaged values computed with program Curves⁵². All distances are in angströms and angles in degrees.

	Xdisp	Inclin	Rise	Twist	RMSD vs A-DNA	RMSD vs B-DNA
A-DNA	-5.4	+19.1	2.6	32.7	0.0	10.7
B-DNA	-0.7	-6.0	3.4	36.0	10.7	0.0
At-A	+0.1	-4.0	3.5	34.2	11.6	5.9
At-B	-0.4	-5.2	3.5	34.5	11.6	6.8
nAt-A	-0.1	-4.2	3.5	34.3	10.6	3.8
nAt-B	-0.1	-4.7	3.5	34.4	11.2	4.1

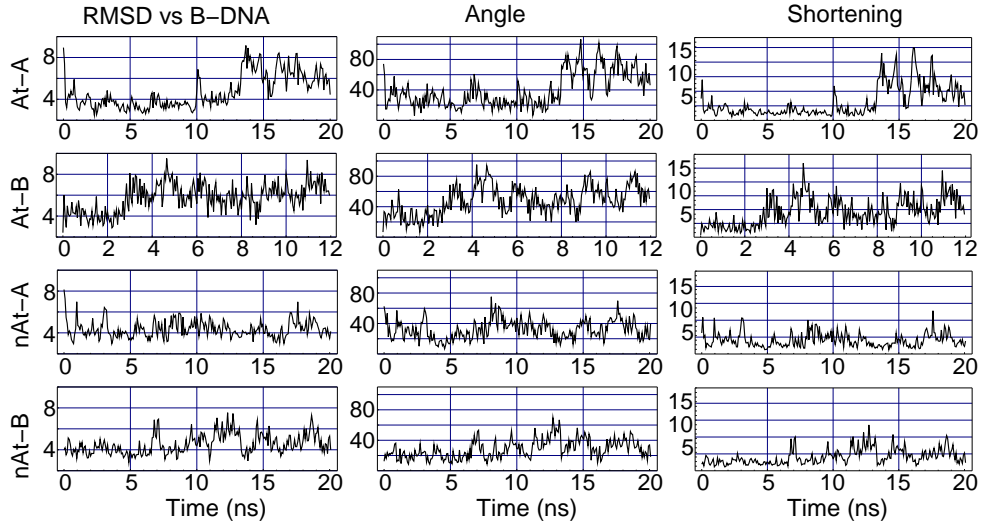


FIG. 2. The time variation of some parameters that characterize the overall DNA shape. The plates are grouped in rows for the same trajectory and in columns for the same parameter. The first column displays the non-hydrogen atom rmsd (in angströms) from the fiber canonical B-DNA⁵¹. The second column shows the bend angle in degrees. The last column shows the shortening, that is the excess length of the curved DNA axis with respect to its end-to-end distance. For example, 10% shortening means that the end-to-end distance is 10% shorter than the curved trace. The traces were smoothed by averaging with a window of 75 ps in At-B and 150 ps otherwise.

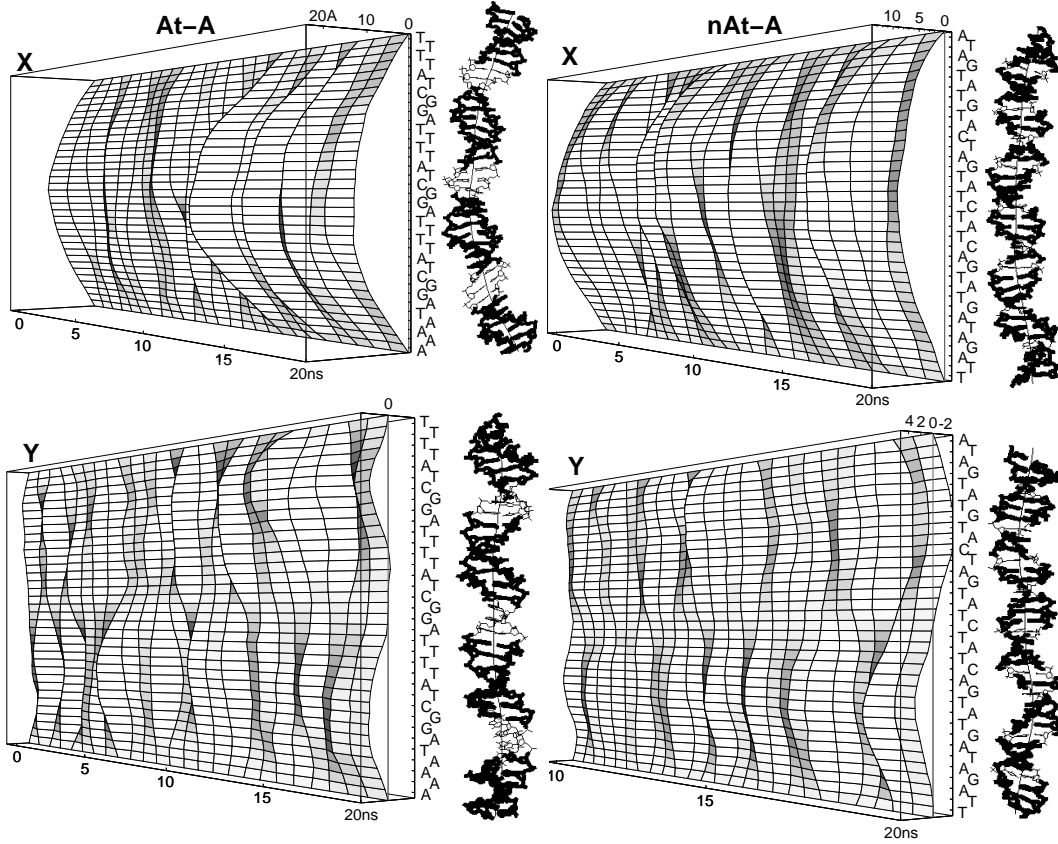


FIG. 3. The time evolution of the overall shape of the helical axis in At-A and nAt-A. The axis of the curved double helix is computed as the best fit common axis of coaxial cylindrical surfaces passing through sugar atoms, which gives solutions close to those produced by the Curves algorithm⁵². The two surface plots labeled **X** and **Y** are constructed by using projections of the curved axis upon the XOZ and YOZ planes, respectively, of the global Cartesian frame shown in Fig. 4a. Any time section of these surfaces gives the corresponding projection averaged over a time window of 400 ps. The horizontal deviation is given in angströms and, for clarity, its relative scale is two times increased with respect to the true DNA length. Shown on the right are the corresponding views of the final 1ns-average conformations. The AT base pairs are shown by thicker lines.

The origin of this difference is analyzed in Fig. 3. It displays dynamics of the overall DNA shape by using two orthogonal projections of the helical axis. A planar bend would give a plane in the **Y** projection and a curved surface in the **X** projection. A sharp increase of curvature in At-A after the 13th nanosecond is evident. Analogous event occurred in At-B after about 3 ns. In agreement with Fig. 2, the two nAt surfaces show fluctuations with amplitudes similar to those during the first 13 ns of At-A. This pattern probably corresponds to a generic type of dynamics characteristic of arbitrary 35-mer DNA fragments.

Comparison of the three columns of plots in Fig. 2 indicates that fluctuations usually occurred simultaneously in all three parameters, which means that the bending dynamics makes a major contribution to the rmsd from B-DNA. Its values shown in Table I are actually much larger than would be for straight conformations with the same helical parameters. For instance, the rmsd between the At-A and At-B structures in Table I was 2.3 Å only because, as we show below, they were bent in the same direction.

Convergence of Trajectories

A DNA molecule with detectable static curvature can either have a minimum of potential energy in a bent state or its energy valley should have a special shape such that a bent form has larger conformational entropy⁵⁷. In both cases such state represents a free energy minimum where MD trajectories should be trapped. The question is, however, how long a real MD trajectory should stay in a bent conformation to be representative. Some experiments suggest that bending dynamics in DNA fragments of only 100 base pairs may involve relaxation times longer than a microsecond^{58,59}, therefore, no practical procedure exists to prove rigorously that computed conformations are representative. Nevertheless, if several trajectories converge to the same state from very different starting points, one can argue that this state is an attractor in the conformational space, which is a necessary condition of the static curvature. The reciprocal convergence of trajectories starting from canonical A- and B-DNA, therefore, is a very important aspect of these simulations. The minimal B-DNA model is not expected to give stable A-DNA structures and we did not try to equilibrate the initial A-DNA states. The start from the A-form is important because it provides an independent dynamic assay with a very different entry to the B-DNA family, which allows one to verify convergence of trajectories to specific conformations. We analyze separately two levels of structural convergence.

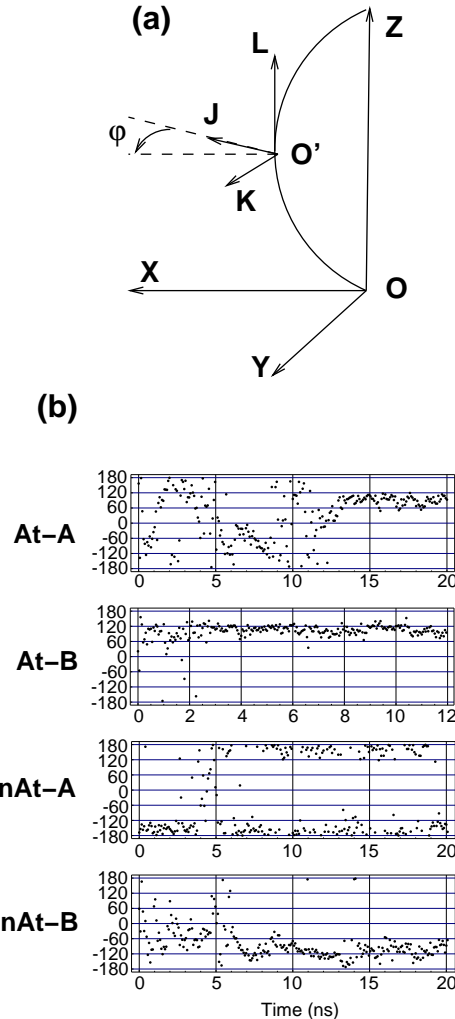


FIG. 4. (a) Geometric constructions used for evaluating the DNA bending. The two coordinate frames shown are the global Cartesian coordinates (OXYZ), and the local frame constructed in the middle point of the curved DNA axis according to the Cambridge convention (O'JKL)⁸⁸. The curve is rotated with two its ends fixed at the Z-axis to put the middle point in plane XOZ. The bending direction is measured by angle φ between this plane and vector **J** of the local frame. By definition, this vector points to the major DNA groove along the short axis of the reference base pair⁸⁸. Consequently, the zero φ value corresponds to the overall bend towards the minor groove in the middle of the DNA fragment. (b) The time evolution of the bending direction as measured by the φ angle in plate (a) (in degrees). The traces have been smoothed by averaging with a window of 75 ps in At-B and 150 ps otherwise.

The rmsd comparison between At-A and At-B is shown in Fig. 5. It clearly demonstrates that At-A and At-B trajectories managed to come very close to each other even though their starting points were significantly separated in conformational space. The initial rmsd of 10.7 Å between the canonical 35-mer A- and B-DNA forms eventually went down to as low as 1.3 Å. The final fall of the rmsd occurred when the curvature drastically increased (compare Figs. 2 and 5). Moreover, during the last nanoseconds the bending direction was virtually identical in At-A and At-B and essentially fixed at around 90° (see Fig. 4b), which explains the origin of the black rectangle in the upper right corner of Fig. 5. This direction corresponds to bending towards the minor groove at approximately three base pair steps from the middle GC pair (see Fig. 4a), that is at the 3' end of the third A-tract in Fig. 1.

The nAt trajectories exhibited qualitatively different features. The rmsd comparison of any two long intervals of nAt-A and nAt-B gives fluctuations between 3 and 6 Å without any clear time trend. Figure 2 shows that the rmsd from B-DNA also fluctuated between 3 and 6 Å and that it correlated with bending parameters. As seen in Fig. 3 the molecule really was not straight. According to Fig. 4b the bending directions in nAt-A and nAt-B were well defined but slightly different. They neither diverged nor converged, remaining at around 100° from each other. The molecule shows no signs of slow straightening, which would give a decrease of fluctuations in Fig. 2 and an increase in scattering of directions in Fig. 4b. All this suggests that bent shapes are favored over straight ones, and that there are many stable bends, with transitions between them being too rare to be sampled by our simulations.

Groove profiles and local structures

Dynamics of the minor groove profiles is shown in Fig. 6. There are evident qualitative resemblance as well as some subtle differences between these four surfaces. In At-B, the characteristic regular groove shape has established early, with significant widenings in the three zones between the A-tracts. The very left widening is somewhat different probably because it occurs between anti-parallel A-tracts. In At-A, the profile strongly changed at the beginning, but also established by the end of the 10th nanosecond. Although the final At-A and At-B profiles are not identical, they are clearly similar, with good correspondence of local widenings and narrowings.

The two nAt surfaces show little similarity between each other, but qualitatively their shapes are not very different from those for the A-tract fragment, with modulations of similar wavelengths and amplitudes. This looks somewhat counter-intuitive because, in experiments, reg-

ular oscillations of the minor groove widths are observed only in A-tract repeats⁶⁰, and this structural periodicity is certainly related to that of the sequence. However, such behavior is exactly what one should expect if the waving of the backbone results from its intrinsic compression. In this case, the groove modulations should occur regardless of the base pair sequence and their characteristic wave lengths should be determined by the backbone stiffness as well as overall helical pitch and diameter. This explains why the waves in the left-hand and the right-hand plates in Fig. 6 have roughly similar scales, even though only the A-tract sequence is periodical. In experiment, however, such modulations can be observed only if their phases are fixed in time, which is the case of A-tract repeats. For random sequences, like the one we use as a reference, the fine structure should be smoothed out on averaging over the whole ensemble.

Figure 7 compares B_I/B_{II} backbone dynamics in the two At trajectories. There are many similarities in dynamics as well as in the final configurations. The convergence is better near both ends and within A-tracts. The dissimilar distributions of the conformers in the middle corresponds to the difference in minor groove profiles in Fig. 6. In A-tracts, the B_{II} conformers are very rare in T-strands and tend to alternate with B_I in A-strands. Figure 8 compares local helical parameters in the last average structures. Only the Buckle and Propeller traces exhibit large scale modulations phased with the helical screw. All parameters strongly fluctuate and these fluctuations are apparently chaotic with rather dissimilar phases in the two structures.

Coupling between the levels

Figures 5 and 4 demonstrate that At-A and At-B arrived at the same statically bent state. This dynamics contrasts those of the two nAt trajectories and it strongly suggest that the curved DNA shape of the A-tract fragment is an attractor of trajectories with a meta-basin of attraction comprising both canonical A and B DNA forms. Figures 6-8 show that the bending convergence is accompanied by some clear trends in local conformational dynamics. These local features are probably coupled to bending, however, a close look reveals that this coupling is very loose. The convergence of the minor groove profiles in Fig. 6 is at best qualitative. Figure 7 indicates that active backbone dynamics continued after the curvature has established and that one can pick up rather different distributions of conformers from the ensemble of bent structures. The noisy traces in Fig. 8 obtained by averaging over two similarly bent ensembles suggest that the helical parameters are far from being constant. The natural conclusion follows that convergence of the bending dynamics does not require unique specific local conformations, i. e. that the bent state is microheterogeneous.

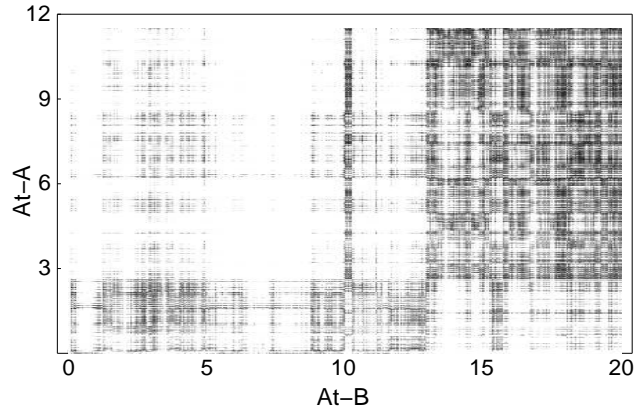


FIG. 5. A 2D density plot of the rms difference between At-A and At-B. Conformations spaced by 2.5 ps intervals were first averaged over of 50 and 25 ps intervals in At-A and At-B, respectively, and the resulting structures compared between the trajectories. Darker shading implies smaller rmsd values. The lower left corner corresponds to the initial structures, that is the canonical A- and B-forms, with rmsd about 10.7 Å. The shaded rectangle in the upper right corner demonstrates convergence of the two trajectories to the same bent state. The values above 4 Å are not shaded whereas in the darkest zones it falls down to 1.3 Å. The black vertical band at approximately 10 ns indicates that At-A shortly visited the final state 3 ns before the definite transition.

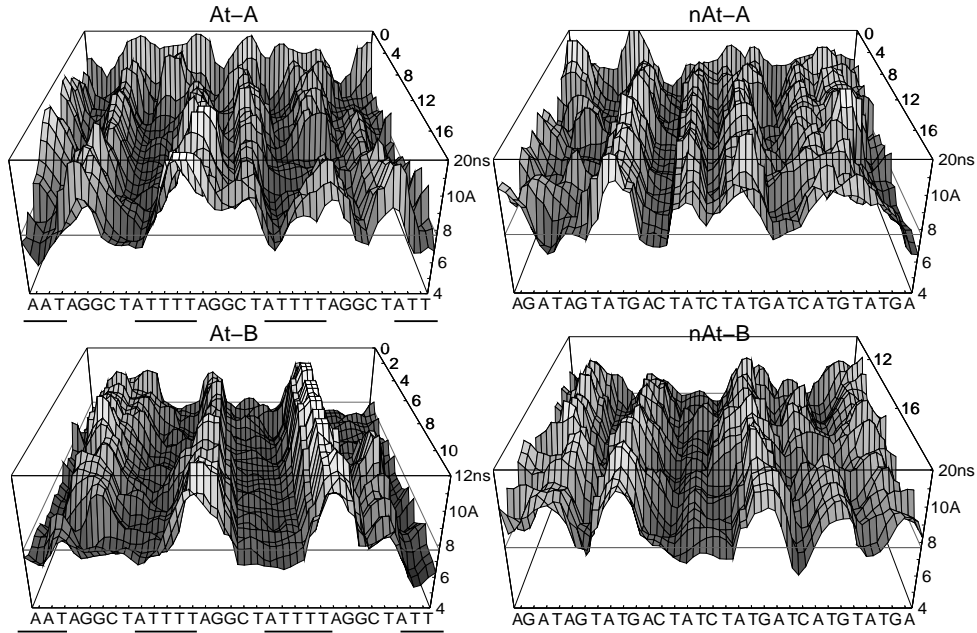


FIG. 6. The time evolution of the profile of the minor groove in the four trajectories. The surface plots are formed by time-averaged successive minor groove profiles, with that on the front face corresponding to the final DNA conformation. The groove width is evaluated by using space traces of C5' atoms⁸⁹. Its value is given in angströms and the corresponding canonical B-DNA level of 7.7 Å is marked by the thin straight lines on the faces of the box. The sequences are shown for the corresponding top strands in Fig. 1 with the 5'-ends on the left. The A-tracts are underlined. Note that the groove width can be measured only starting from the third base pair from both termini.

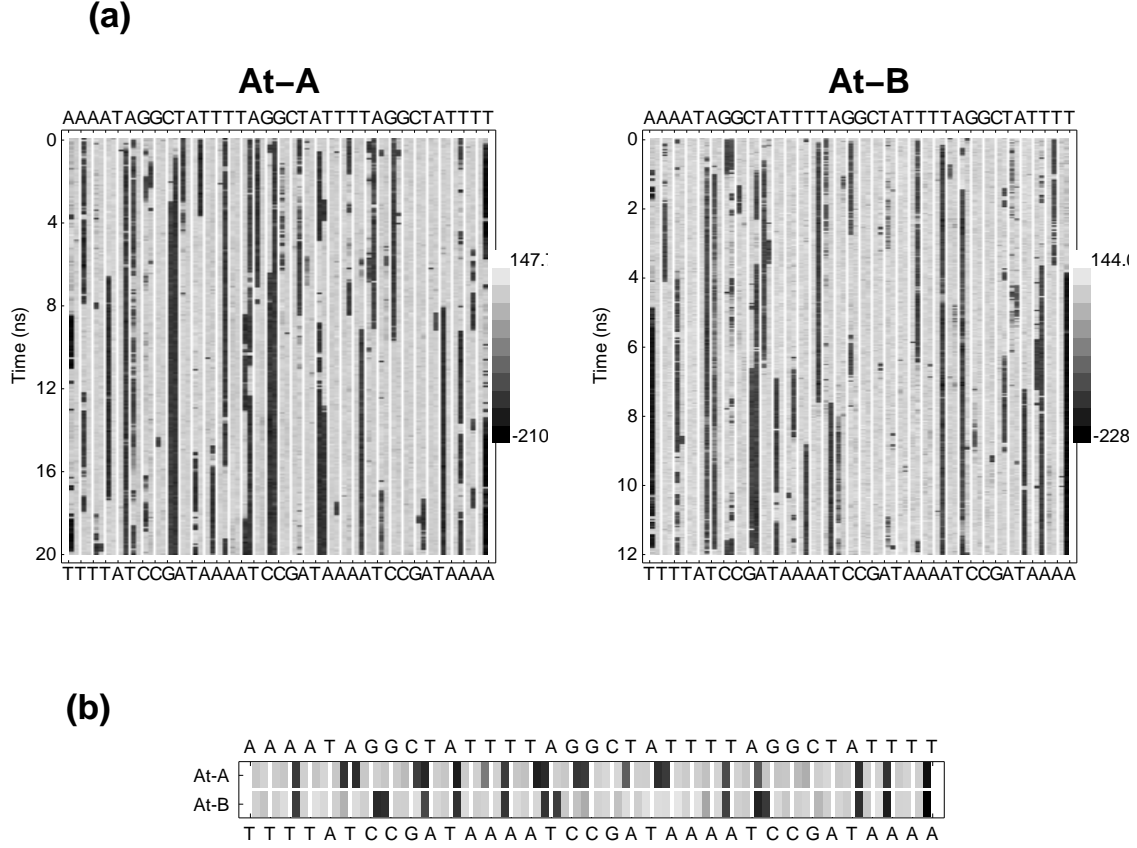


FIG. 7. (a) Dynamics of B_I and B_{II} backbone conformers in At-A and At-B. The B_I and B_{II} conformations are distinguished by the values of two consecutive backbone torsions, ε and ζ . In a transition, they change concertedly from (t, g^-) to (g^-, t) . The difference $\zeta - \varepsilon$ is, therefore, positive in B_I state and negative in B_{II} , and it is used as a monitoring indicator, with the corresponding gray scale levels shown on the right. Each base pair step is characterized by a column consisting of two sub-columns, with the left sub-columns referring to the sequence written at the top in 5'-3' direction from left to right. The right sub-columns refer to the complementary sequence shown at the bottom. (b) Comparison of the final distributions of B_I and B_{II} backbone conformers in At-A and At-B shown in the same way as in plate (a).

The Magnitude and The Character of Bending in the A-tract Repeat

The experimental magnitude of bending caused by A-tracts was earlier estimated by several groups with different approaches^{61,21,62,32}. The reported bend angles were between 11° and 28° per A-tract, and 18° is presently considered as the most reasonable estimate⁹. The curvature somewhat varies with the base pair sequence and depends upon environmental conditions such as the temperature, the concentration of counterions etc. Although in calculations all these details cannot yet be properly taken into account a quantitative comparison with experiment is instructive.

When the curvature has established, that is after 13 ns of dynamics in At-A and after 3 ns in At-B, the bend angle oscillated around 60° (see Fig. 2). In the consecutive 1ns-averaged conformations its value was between 42° and 74° , with the average of 54° for 16 such structures. This value corresponds to $54/4=13.5^\circ$ per A-tract, that is close to the lower experimental estimate. A larger value of $54/3=18^\circ$ results, however, if one assumes, as suggested by some experimental observations^{23,63} that the A-tracts are straight, and that the bending actually occurs in the three zones between them. Yet another estimate is obtained from the increase of bending with respect to the shorter 25-mer fragment studied earlier²⁵. It appears that one additional A-tract and junction zone increase the overall bend by $20\text{--}22^\circ$. We see that the magnitude of bending in simulations is rather close to experimental estimates, and that the agreement is better if the curvature is really localized in the junction zones between A-tracts.

Figure 9 presents a closer look at how the local curvature is distributed in the last 1-ns average structure of At-B. The total bending angle is about 50° . Three zones contribute more than other to the overall bend. The two junctions between A-tracts 2, 3 and 4 are bent in an identical direction which is close to that of the whole structure. Together they contribute around 40° to the total bend, which is the largest local positive contribution. In contrast, the strongly curved fourth A-tract makes a negative contribution because its direction diverges by more than 90° . The third A-tract is virtually straight. Finally, A-tracts 1 and 2 and the junction zone between them exhibit a smooth curvature with a stable “good” direction and contribute the remaining 20° of the total bend.

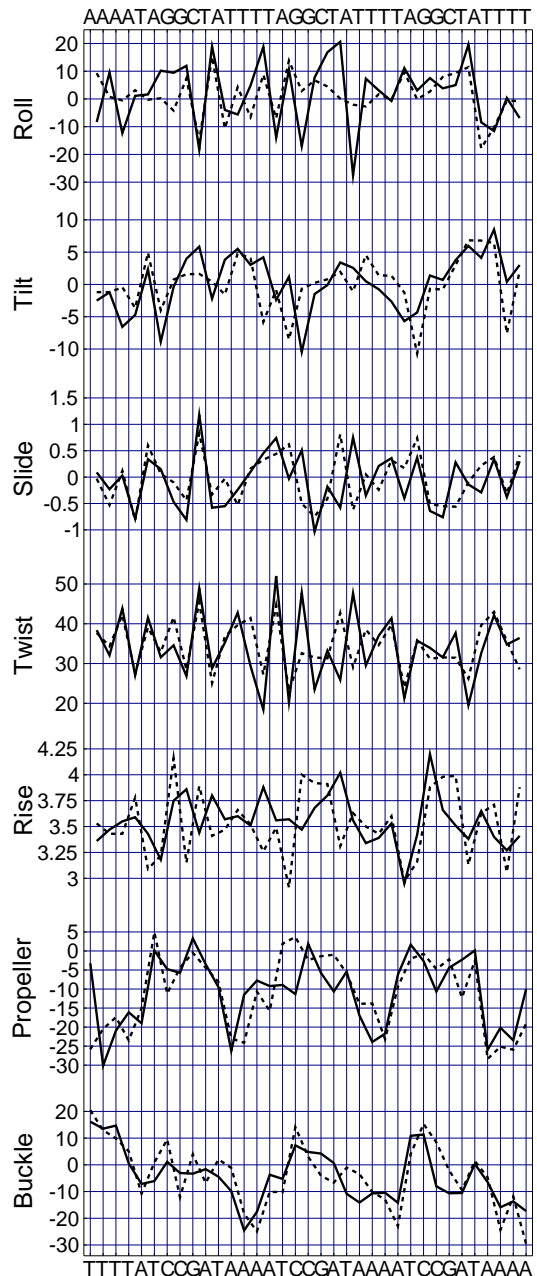


FIG. 8. Sequence variations of helicoidal parameters in the last 1ns-averaged structures of At-A and At-B. The sequence of the first strand is shown on the top in 5' – 3' direction. The complementary sequence of the second strand is written on the bottom in the opposite direction. All parameters were evaluated with the Curves program⁵² and are given in degrees and angstroms. At-A – solid line, At-B – dashed line.

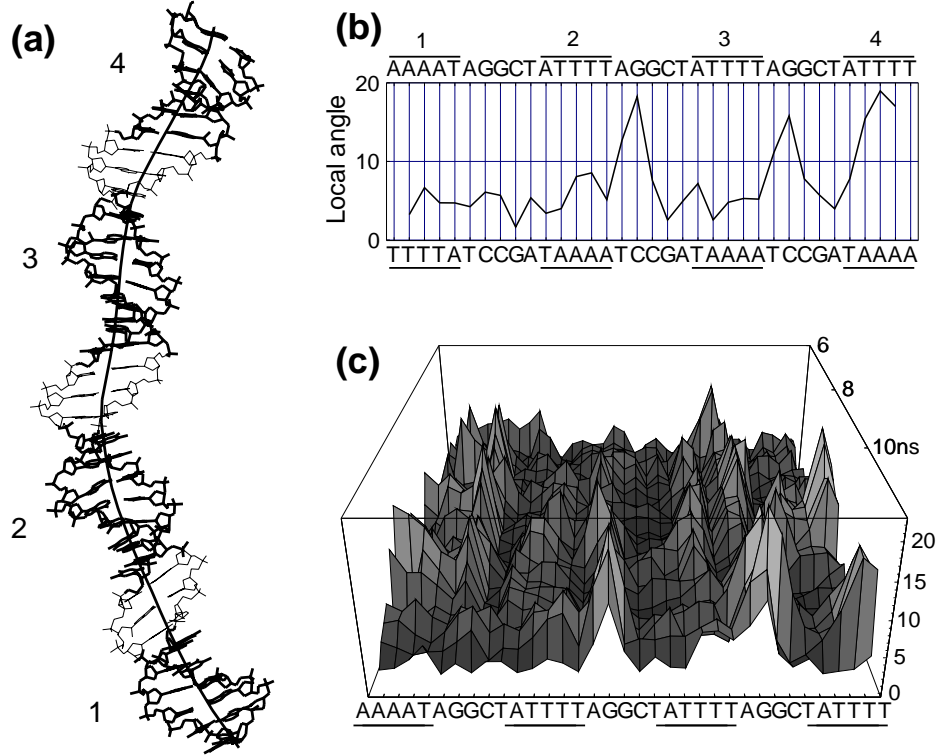


FIG. 9. (a) The last 1-ns average structure of At-B shown in the XOZ projection according Fig. 4a. The AT base pairs are highlighted. (b) The quantified distribution of curvature in the structure shown in plate (a). The local bending angle is evaluated by moving a sliding window along the helical axis. The window size was 3 base pair steps, with the measured values assigned to its center. The sequences of strands are given as in Fig. 1 with the A-tracts underlined and numbered. (c) Dynamics of local bending in At-B. The surface plot is formed by time-averaged successive profiles like that in plate (b), with the front face of the box corresponding to the end of the trajectory.

The foregoing analysis certainly is not free from pitfalls. For instance, the apparent smooth curvature can result from time averaging of several alternative local bends. Nevertheless, Fig. 9 indicates that there are zones in this DNA fragment that are bent more than other and that two such zones are distinguishable between A-tracts. Figure 9c displays the local bending dynamics in At-B. It is seen that the main features noticed in plates (a) and (b) were quite visible during the whole trajectory. Moreover, the zone between the first two A-tracts also sometimes carried an increased curvature. However, it would be incorrect to conclude that A-tracts are straight. They just exhibit generally smaller and distributed curvature than the junction zones. This curvature is usually directed towards the minor groove, therefore, it does not cancel out in averaged structures.

The foregoing pattern agrees qualitatively with the recent NMR⁶⁴ and X-ray data⁶⁵ as well as the character of bending earlier observed in calculations^{39,40}. Many earlier reported X-ray structures of A-tracts suggested that they produce an intrinsically straight DNA compared to other sequences⁶³. Our calculations do not contradict these observations because the crystal A-tract structures should be additionally straightened due to special crystallization conditions^{30,31,66}, and because a single short A-tract may in fact be somewhat less curved than that inserted in a long DNA fragment.

Verification of Curvature by Gel Electrophoresis

The sequence induced static DNA curvature was first noticed owing to reduced migration rate of curved DNA fragments in gel electrophoresis¹. Later gel migration studies provided a wealth of information on curvature in A-tract repeats⁷. The difference in gel mobility between straight and curved DNA rapidly grows with chain length, therefore, the curvature was usually studied in rather long DNA fragments. Data for sequences shorter than 50 bp are rare²⁷, and, to our best knowledge, it has never been shown that curved and straight 35-mers could be distinguished. Nevertheless, subtle sequence effects in double stranded oligomers of around 10 bp were detected with higher gel concentration⁶⁷, and one could hope that this would work for somewhat longer sequences as well. Alternatively, the effect of bending could be enhanced by inserting constructed fragments into a long stretch of straight DNA², but this would complicate further analysis because the DNA molecules used in experiments and calculations could no longer be identical.

Figure 10 shows comparison of the acrylamide gel mobility of these two fragments. As expected, the A-tract repeat exhibits a reduced rate of migration. The difference is quite significant so that the two molecules are well resolved both in separate lanes and when mixed in the same sample. Owing to the identical base pair content, the minor factors such as the number of tightly bound

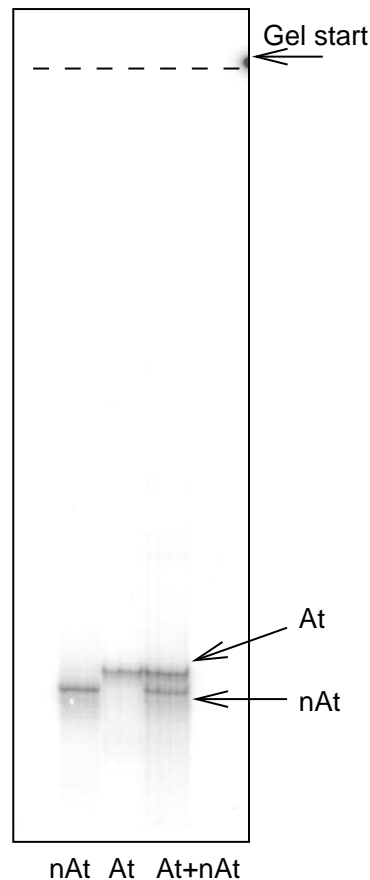


FIG. 10. Gel mobility assay. The two ³²P-labeled 35 bp DNA constructs (At and nAt) were electrophoresed in 16% polyacrylamide gel buffered with Tris-borate, pH 8.6. The gel was dried and autoradiographed. The lanes labeled At, nAt, and At+nAt correspond to the A-tract repeat, the random sequence, and their mixture, respectively. Bands assigned to each DNA fragment are marked by arrows.

counterions and water molecules is reduced here to the possible minimum and, most probably, the observed difference is entirely due to the curvature in the A-tract fragment.

DISCUSSION

Comparison with Earlier Studies

To our knowledge, the only earlier successful unbiased simulations aimed at reproducing A-tract induced curvature in DNA have been reported by David Beveridge group^{39,40}. These simulations were carried out in full water environment with explicit counterions. The character of the phased A-tract bending appeared oscillatory with a period of at least 3 to 4 ns³⁹. Because duration of trajectories was only 5 ns, it was difficult to confirm the static character of bending and distinguish between essential and occasional observations. Therefore, conclusions concerning applicability of different models were not restrictive and left room for many theories. Our simulations have the same goal and a similar set up, but we use a simpler model system. The primarily long term interest in B-DNA models with implicit or semi-implicit representation of environment is connected with approximate simulations of very long DNA molecules³⁸. As shown here the minimal model can also capture, at least qualitatively, important sequence effects like the A-tract induced curvature.

Several features in our calculations correspond well to those observed earlier, notably, spontaneous development of quasi-sinusoidal minor groove profiles in both A-tract and non-A-tract sequences and strong bends in junction zones between A-tracts. In contrast to earlier simulations, however, the curvature here emerged after several nanoseconds of dynamics and the difference between the A-tract and non-A-tract structures did not reduce with time. One should note also that the A-tract structures computed with the minimal model are very close to experimental data as regards the helical pitch and the absolute groove sizes^{25,50}. In standard AMBER and CHARMM simulations, B-DNA always appears somewhat underwound and the narrowest A-tract minor grooves remain 1-2 Å wider than in experimental structures^{39,40,42}. The origin of this subtle bias remains unclear, and attempts to reduce it have been made in the very recent modifications of the AMBER force field^{47,68}. In the minimal model, this bias was compensated by fitting reduced phosphate charges, which apparently improved the A-tract structures and stabilized the curvature.

A significant enforcement of the present results compared to our previous reports^{25,54} consists in the direct comparison of bending *in silico* and *in vitro*, which became possible owing to increased length of the DNA fragment. Such a possibility is rather unique for MD simula-

tions and we believe this approach presents considerable interest for future studies. Sequence effects in DNA fragments of 35-50 base pairs can be probed in both MD simulations and gel electrophoresis. Such experiments are rapid and inexpensive, which progressively becomes the case for MD simulations as well.

Comparison with Theories of DNA Bending

The origin of intrinsic curvature in DNA remains unclear. Theories that explain it always assume some specific balance of interactions in the DNA structure, and that is why these theories are perhaps more important than the particular role of A-tracts. The list of available interactions is well-known, but the question is which of them is the driving force. Below we briefly analyze our results in contexts of some theories.

Base Pair Stacking Models

According to any mechanism that starts from base pair stacking, like the wedge or the junction models^{12,18,2}, a curved DNA must be built out of asymmetric blocks, with their structures determined by base pair sequence. The bending, therefore, must be accompanied by repetition of local structures in identical sequence fragments. This fundamental theoretical prediction fails for the static bends observed here, which confirms earlier conclusions^{25,54}. The structures of sequence repeats in the bent state are microscopically heterogeneous and convergence to specific local conformations is not necessary for bending. As shown above, the A-tract trajectories arrive at a single bent state, but the minor groove profiles in Fig. 6 are only similar, not identical as well as local helical parameters and backbone conformations in Figs. 7 and 8.

Counterion Electrostatic Models

An alternative model that recently attracted much attention considers solvent cations trapped in A-tract minor grooves as the initial cause of bending²⁴. The role of counterions in this phenomenon is rather controversial^{69,65,70}, and a few general comments are necessary before considering our results. Because straight DNA structures correspond to symmetric minima of electrostatic energy bends can result from symmetry breaking in the charge distribution, namely, if positive external charges accumulate at one DNA side it should bend towards them^{71,72,73,74,24}. However, the same situation is well interpreted by other models of bending. Namely, in a curved double helix, the phosphate groups at the inner edge must approach, which creates regions of low potential that should be populated by counterions if they

are available⁶¹. In the first case the counterion-DNA interactions are sequence specific and they cause bending. In the second case they are structure specific and they stabilize pre-existing curvature.

Two physically different models of sequence-specific counterion involvement can be distinguished. In the first one the counterions act locally. When a counterion is placed in one of the DNA grooves between two phosphate groups their electrostatic interaction becomes attractive, which narrows the groove⁷⁴. As in some earlier models^{75,60}, the global curvature results from a general mechanical link between groove deformations and bending. In contrast, the second model is purely electrostatic. Here the minor grooves of A-tracts act as flexible ionophores^{24,76} and trap counterions. Since in phased sequences they occur at the same DNA side the double helix bends towards them to relax the long range phosphate repulsion at the opposite side.

The second model employs the general idea initially proposed for protein DNA interactions⁷¹ and confirmed experimentally for free DNA⁷². However, it qualitatively disagrees with a cornerstone experimental observation concerning the A-tract induced bending, namely, that an A-tract can be characterized by a definite bend angle regardless of its length and the distance from other A-tracts. When the length of an A-tract exceeds one helical turn both sides of the double helix appear neutralized. As a result, the curvature should decrease in the series $(A_{12}N_9)_n - (A_{14}N_7)_n - (A_{16}N_5)_n$ because the length of the non-neutralized N-tracts is reduced, and furthermore, in sequence $(A_{16}N_5)_n$ the bend angle per A-tract should be drastically reduced with respect to that in $(A_6N_5)_n$, for example, because the distance between the repulsive N-tracts is increased. These predictions apparently disagree with the experimental trends⁷⁷ although additional experiments are perhaps necessary to check them.

The first model cannot explain the origin of the A-tract curvature because only multivalent counterions can cause significant bends⁷⁴ whereas bending is commonly observed in buffers containing EDTA and other chelating agents. Also, the optimal counterion position for this type of bend is at the entrance of the groove and not inside, therefore, it cannot be both strong and sequence specific. The last argument agrees with the recent MD studies of correlations between the minor groove width and positioning of counterions. Notably, there is no such correlation when only counterions interacting with bases are considered⁷⁰. In contrast, a correlation exists for counterion positions at the groove entrance⁷⁸. The last observation corresponds to the structure specific binding better than to the sequence specific one. Structure-specific interactions can explain all experimental results concerning the preferential binding of counterions in A-tracts^{79,24,80}, which makes such data intrinsically neutral as regards different models of bending.

In our calculations all counterion effects are considered non-specific, and the results obtained indicate that modulations of DNA grooves and static bending are phys-

ically possible without breaking the charge symmetry around DNA. Although simulations alone cannot prove the real mechanism all experimental and computational observations taken together suggest that solvent counterions are hardly responsible for the intrinsic curvature in DNA, which by no means questions their important role in DNA structure and function.

Compressed Backbone Theory

The main idea of the compressed backbone theory²⁵ was outlined in Introduction. All seemingly paradoxical MD observations from which it originally emerged are confirmed here. Notably, this theory predicts that, with any base pair sequence, the backbone stiffness should cause smooth modulations of DNA grooves. The helical symmetry becomes broken with the base pair stacking perturbed, which creates regions of intrinsic curvature. In a “random” DNA, the local curvature changes its direction with time because groove widenings and narrowings migrate slowly along the double helix. As a result, the generic DNA appears straight on average although it is curved locally. In sequences where certain base pair properties strongly alternate, the phases of backbone oscillations appear fixed. In this case the local curvature can sum up to give macroscopic static bends, as in A-tract repeats. This theory considers a macroscopically curved DNA as an “idioform” characterized by topological attributes, rather than a structure with fixed atom positions. These attributes are the bend direction and the phase of groove modulations. The microheterogeneity of the bent state should be expected because the same waving backbone profile is compatible with many alternative local conformations.

A competition between the stacking interactions and the backbone compression postulated by this theory is characteristic of physical systems called frustrated⁸¹. Consider the common textbook example of three anti-ferromagnetic spins in a triangle configuration. The optimal orientation of each pair is anti-parallel, but all three pairs cannot be anti-parallel in a triangle. There is always at least one parallel pair and the ground state appears degenerate. Now consider a circular duplex DNA with a homopolymer sequence. The compressed backbone causes groove modulations, but there are no preferable regions for narrowings and widenings and the ground state appears strongly degenerate. The similarity between these two examples is evident. One usual physical consequence of frustration is very important for biology, namely, the possibility of a glassy state where microscopic transitions are dramatically slowed down. Transitions between wavy backbone configurations in a long DNA can be very slow because many groove narrowings and widenings must be moved concertedly. This may explain observations of supra-microsecond relaxation times in bending dynamics of relatively short DNA fragments^{58,59}.

Finally, the compressed backbone theory offers a new view of some environmental effects upon the curvature. Common physical factors like the temperature, counterions, and various dehydrating agents are long-known to change slightly the helical pitch of DNA^{82,83,84}, which can reasonably be attributed to the dependence of the state of the DNA backbone upon the solvent screening of phosphates. These same factors modulate significantly the sequence specificity of nucleases probably by changing the shape of DNA grooves⁸⁵, and produce complex effects upon the intrinsic curvature^{26,27,29,30,31,28}. It seems wise to postpone any detailed interpretation of these facts for future studies, but one can just note that with intrinsic frustration outlined above a very small change in the partial specific backbone length can induce significant global changes in the DNA structure.

Possibilities of Experimental Verification of Backbone Compression

The the compressed backbone theory does not give simple rules for *a priori* calculation of curvature in any sequence. Nevertheless, it offers some predictions that can be checked in experiments. It suggests, for example, that the A-tract curvature can be relaxed by introducing single-strand breaks. It seems interesting also to examine the possible relationship between the backbone compression and supercoiling. There is a consensus that intrinsic bends affect the shape of the superhelical DNA^{86,87}. Unlike other models, however, the compressed backbone theory predicts that the intrinsic curvature should vary under superhelical stress in a rather special way. Namely, with a positive density, the backbone is stretched and the curvature of an internal A-tract repeat should be reduced. Conversely, the curvature should increase when the superhelical density is negative. Diekmann and Wang earlier observed that the A-tract structure changes under superhelical stress²⁶, and their approach may serve for a more specific experimental verification of the above predictions.

¹ J. C. Marini, S. D. Levene, D. M. Crothers, and P. T. Englund, Bent helical structure in kinetoplast DNA, *Proc. Natl. Acad. Sci. USA* **79**, 7664 (1982).

² H.-M. Wu and D. M. Crothers, The locus of sequence-directed and protein-induced DNA bending, *Nature* **308**, 509 (1984).

³ P. J. Hagerman, Evidence for the existence of stable curvature of DNA in solution, *Proc. Natl. Acad. Sci. USA* **81**, 4632 (1984).

- ⁴ S. Diekmann, in *Nucleic Acids and Molecular Biology*, Vol. 1, edited by F. Eckstein and D. M. J. Lilley (Springer-Verlag, Berlin Heidelberg, 1987), pp. 138–156.
- ⁵ P. J. Hagerman, Sequence-directed curvature of DNA, *Annu. Rev. Biochem.* **59**, 755 (1990).
- ⁶ D. M. Crothers, T. E. Haran, and J. G. Nadeau, Intrinsically bent DNA, *J. Biol. Chem.* **265**, 7093 (1990).
- ⁷ D. M. Crothers and J. Drak, Global features of DNA structure by comparative gel electrophoresis, *Meth. Enzymol.* **212**, 46 (1992).
- ⁸ W. K. Olson and V. B. Zhurkin, in *Structure and Dynamics. Vol. 2: Proceedings of the Ninth Conversation, State University of New York, Albany, NY 1995*, edited by R. H. Sarma and M. H. Sarma (Adenine Press, New York, 1996), pp. 341–370.
- ⁹ D. M. Crothers and Z. Shakked, in *Oxford Handbook of Nucleic Acid Structure*, edited by S. Neidle (Oxford University Press, New York, 1999), pp. 455–470.
- ¹⁰ N. Z. Namoradze, A. N. Goryunov, and T. M. Birshstein, On conformations of the superhelix structure, *Biophys. Chem.* **7**, 59 (1977).
- ¹¹ V. B. Zhurkin, Y. P. Lysov, and V. I. Ivanov, Anisotropic flexibility of DNA and the nucleosomal structure, *Nucl. Acids Res.* **6**, 1081 (1979).
- ¹² E. N. Trifonov and J. L. Sussman, The pitch of chromatin DNA is reflected in its nucleotide sequence, *Proc. Natl. Acad. Sci. USA* **77**, 3816 (1980).
- ¹³ P. De Santis, A. Palleschi, M. Savino, and A. Scipioni, Validity of the nearest-neighbor approximation in the evaluation of the electrophoretic manifestations of DNA curvature, *Biochemistry* **29**, 9269 (1990).
- ¹⁴ A. Bolshoy, P. McNamara, R. E. Harrington, and E. N. Trifonov, Curved DNA without A-A. Experimental estimation of all 16 DNA wedge angles, *Proc. Natl. Acad. Sci. USA* **88**, 2312 (1991).
- ¹⁵ Y. Liu and D. L. Beveridge, A refined prediction method for gel retardation of DNA oligonucleotides from dinucleotide step parameters: Reconciliation of DNA bending models with crystal structure data, *J. Biomol. Struct. Dyn.* **18**, 505 (2001).
- ¹⁶ M. Dlakić and R. E. Harrington, The effects of sequence context on DNA curvature, *Proc. Natl. Acad. Sci. USA* **93**, 3847 (1996).
- ¹⁷ M. Dlakić and R. E. Harrington, Unconventional helical phasing of repetitive DNA motifs reveals their relative bending contributions, *Nucl. Acids Res.* **26**, 4274 (1998).
- ¹⁸ S. D. Levene and D. M. Crothers, A computer graphics study of sequence-directed bending of DNA, *J. Biomol. Struct. Dyn.* **1**, 429 (1983).
- ¹⁹ E. Selsing, R. D. Wells, C. J. Alden, and S. Arnott, Bent DNA: Visualization of a base-paired and stacked A-B conformational junctions, *J. Biol. Chem.* **254**, 5417 (1979).
- ²⁰ D. G. Alexeev, A. A. Lipanov, and I. Y. Skuratovskii, Poly(dA).poly(dT) is a B-type double helix with a distinctively narrow minor groove, *Nature* **325**, 821 (1987).
- ²¹ C. R. Calladine, H. R. Drew, and M. J. McCall, The intrinsic curvature of DNA in solution, *J. Mol. Biol.* **201**, 127 (1988).
- ²² R. C. Maroun and W. K. Olson, Base sequence effects in double-helical DNA. III. Average properties of curved

- DNA, *Biopolymers* **27**, 585 (1988).
- ²³ R. E. Dickerson, D. S. Goodsell, and S. Neidle, '... the tyranny of the lattice ...', *Proc. Natl. Acad. Sci. USA* **91**, 3579 (1994).
 - ²⁴ N. V. Hud, V. Sklenář, and J. Feigon, Localization of ammonium ions in the minor groove of DNA duplexes in solution and the origin of DNA A-tract bending, *J. Mol. Biol.* **286**, 651 (1999).
 - ²⁵ A. K. Mazur, Theoretical studies of the possible origin of intrinsic static bends in double helical DNA, *J. Am. Chem. Soc.* **122**, 12778 (2000).
 - ²⁶ S. Diekmann and J. C. Wang, On the sequence determinants and flexibility of the kinetoplast DNA fragment with abnormal gel electrophoretic mobilities, *J. Mol. Biol.* **186**, 1 (1985).
 - ²⁷ S. Diekmann, Temperature and salt dependence of gel migration anomaly of curved DNA fragments, *Nucl. Acids Res.* **15**, 247 (1987).
 - ²⁸ B. Jerkovic and P. H. Bolton, The curvature of dA tracts is temperature dependent, *Biochemistry* **39**, 12121 (2000).
 - ²⁹ J. C. Marini, P. N. Effron, T. C. Goodman, C. K. Singleton, R. D. Wells, R. M. Wartell, and P. T. Englund, Physical characterization of a kinetoplast DNA fragment with unusual properties, *J. Biol. Chem.* **259**, 8974 (1984).
 - ³⁰ D. Sprous, W. Zacharias, Z. A. Wood, and S. C. Harvey, Dehydrating agents sharply reduce curvature in DNAs containing A tracts, *Nucl. Acids Res.* **23**, 1816 (1995).
 - ³¹ M. Dlakic, K. Park, J. D. Griffith, S. C. Harvey, and R. E. Harrington, The organic crystallizing agent 2-methyl-2,4-pentanediol reduces DNA curvature by means of structural changes in A-tracts, *J. Biol. Chem.* **271**, 17911 (1996).
 - ³² H.-S. Koo, J. Drak, J. A. Rice, and D. M. Crothers, Determination of the extent of DNA bending by an adenine-thymine tract, *Biochemistry* **29**, 4227 (1990).
 - ³³ N. B. Ulyanov and V. B. Zhurkin, Sequence-dependent anisotropic flexibility of B-DNA: A conformational study, *J. Biomol. Struct. Dyn.* **2**, 361 (1984).
 - ³⁴ S. R. Sanghani, K. Zakrzewska, S. C. Harvey, and R. Lavery, Molecular modelling of $(A_4T_4NN)_n$ and $(T_4A_4NN)_n$: Sequence elements responsible for curvature, *Nucl. Acids Res.* **24**, 1632 (1996).
 - ³⁵ E. von Kitzing and S. Diekmann, Molecular mechanics calculations of dA_{12} , dT_{12} and of the curved molecule $d(GCTCGAAAA)_4$, $d(TTTTTCGAGC)_4$, *Eur. Biophys. J.* **14**, 13 (1987).
 - ³⁶ V. P. Chuprina and R. A. Abagyan, Structural basis of stable bending in DNA containing A_n tracts. Different types of bending, *J. Biomol. Struct. Dyn.* **6**, 121 (1988).
 - ³⁷ V. B. Zhurkin, N. B. Ulyanov, A. A. Gorin, and R. L. Jernigan, Static and statistical bending of DNA evaluated by Monte Carlo simulations, *Proc. Natl. Acad. Sci. USA* **88**, 7046 (1991).
 - ³⁸ T. E. Cheatham, III and P. A. Kollman, Molecular dynamics simulations of nucleic acids, *Annu. Rev. Phys. Chem.* **51**, 435 (2000).
 - ³⁹ M. A. Young and D. L. Beveridge, Molecular dynamics simulations of an oligonucleotide duplex with adenine tracts phased by a full helix turn, *J. Mol. Biol.* **281**, 675 (1998).
 - ⁴⁰ D. Sprous, M. A. Young, and D. L. Beveridge, Molecular dynamics studies of axis bending in $d(G_5 - (GA_4T_4C)_2 - C_5)$ and $d(G_5 - (GT_4A_4C)_2 - C_5)$: Effects of sequence polarity on DNA curvature, *J. Mol. Biol.* **285**, 1623 (1999).
 - ⁴¹ E. C. Sherer, S. A. Harris, R. Soliva, M. Orozco, and C. A. Laughton, Molecular dynamics studies of DNA A-Tract structure and flexibility, *J. Am. Chem. Soc.* **121**, 5981 (1999).
 - ⁴² D. Strahs and T. Schlick, A-tract bending: Insights into experimental structures by computational models, *J. Mol. Biol.* **301**, 643 (2000).
 - ⁴³ A. K. Mazur, Quasi-Hamiltonian equations of motion for internal coordinate molecular dynamics of polymers, *J. Comput. Chem.* **18**, 1354 (1997).
 - ⁴⁴ A. K. Mazur, in *Computational Biochemistry and Biophysics*, edited by O. M. Becker, A. D. MacKerell, Jr, B. Roux, and M. Watanabe (Marcel Dekker, New York, 2001), pp. 115–131.
 - ⁴⁵ A. K. Mazur, Symplectic integration of closed chain rigid body dynamics with internal coordinate equations of motion, *J. Chem. Phys.* **111**, 1407 (1999).
 - ⁴⁶ W. D. Cornell, P. Cieplak, C. I. Bayly, I. R. Gould, K. M. Merz, D. M. Ferguson, D. C. Spellmeyer, T. Fox, J. W. Caldwell, and P. A. Kollman, A second generation force field for the simulation of proteins, nucleic acids and organic molecules, *J. Am. Chem. Soc.* **117**, 5179 (1995).
 - ⁴⁷ T. E. Cheatham, III, P. Cieplak, and P. A. Kollman, A modified version of the Cornell et al. force field with improved sugar pucker phases and helical repeat, *J. Biomol. Struct. Dyn.* **16**, 845 (1999).
 - ⁴⁸ W. L. Jorgensen, Transferable intermolecular potential functions for water, alcohols and ethers: Application to liquid water., *J. Am. Chem. Soc.* **103**, 335 (1981).
 - ⁴⁹ A. K. Mazur, Accurate DNA dynamics without accurate long range electrostatics, *J. Am. Chem. Soc.* **120**, 10928 (1998).
 - ⁵⁰ A. K. Mazur, Molecular dynamics of minimal B-DNA, *J. Comput. Chem.* **22**, 457 (2001).
 - ⁵¹ S. Arnott and D. W. L. Hukins, Optimised parameters for A-DNA and B-DNA, *Biochem. Biophys. Res. Commun.* **47**, 1504 (1972).
 - ⁵² R. Lavery and H. Sklenar, The definition of generalized helicoidal parameters and of axis curvature for irregular nucleic acids, *J. Biomol. Struct. Dyn.* **6**, 63 (1988).
 - ⁵³ P. Tuffery, Xmol: An X11 and motif program for macromolecular visualization and modelling, *J. Mol. Graph.* **13**, 67 (1995).
 - ⁵⁴ A. K. Mazur, Molecular dynamics studies of sequence-directed curvature in bending locus of trypanosome kinetoplast DNA, *J. Biomol. Struct. Dyn.* **18**, 832 (2001).
 - ⁵⁵ H.-S. Koo, H.-M. Wu, and D. M. Crothers, DNA bending at adenine-thymine tracts, *Nature* **320**, 501 (1986).
 - ⁵⁶ W. Kabsch, C. Sander, and E. N. Trifonov, The ten helical twist angles for B-DNA, *Nucl. Acids Res.* **10**, 1097 (1982).
 - ⁵⁷ W. K. Olson, N. L. Marky, R. L. Jernigan, and V. B. Zhurkin, Influence of fluctuation on DNA curvature: A comparison of flexible and static wedge models of intrinsically bent DNA, *J. Mol. Biol.* **232**, 530 (1993).
 - ⁵⁸ L. Song and J. M. Schurr, Dynamic bending rigidity of DNA, *Biopolymers* **30**, 229 (1990).
 - ⁵⁹ T. M. Okonogi, A. W. Reese, S. C. Alley, P. B. Hopkins, and R. H. Robinson, Flexibility of duplex DNA on the sub-

- microsecond timescale, *Biophys. J.* **77**, 3256 (1999).
- ⁶⁰ A. M. Burkhoff and T. D. Tullius, The unusual conformation adopted by the adenine tracts in kinetoplast DNA, *Cell* **48**, 935 (1987).
 - ⁶¹ S. D. Levene, H.-M. Wu, and D. M. Crothers, Bending and flexibility of kinetoplast DNA, *Biochemistry* **25**, 3988 (1986).
 - ⁶² L. E. Ulanovsky, M. Bodner, E. N. Trifonov, and M. Choder, Curved DNA: Design, synthesis, and circularization, *Proc. Natl. Acad. Sci. USA* **83**, 862 (1986).
 - ⁶³ M. A. Young, G. Ravishanker, D. L. Beveridge, and H. M. Berman, Analysis of local helix bending in crystal structures of DNA oligonucleotides and DNA-protein complexes, *Biophys. J.* **68**, 2454 (1995).
 - ⁶⁴ D. MacDonald, K. Herbert, X. Zhang, T. Polgruto, and P. Lu, Solution structure of an A-tract DNA bend, *J. Mol. Biol.* **306**, 1081 (2001).
 - ⁶⁵ T. K. Chiu, M. Zaczor-Grzeskowiak, and R. E. Dickerson, Absence of minor groove monovalent cations in the crosslinked dodecamer C-G-C-G-A-A-T-T-C-G-C-G, *J. Mol. Biol.* **292**, 589 (1999).
 - ⁶⁶ R. E. Dickerson, D. Goodsell, and M. L. Kopka, MPD and DNA bending in crystals and in solution, *J. Mol. Biol.* **256**, 108 (1996).
 - ⁶⁷ J.-H. Chen, N. C. Seeman, and N. R. Kallenbach, Tracts of AT base pairs retard the electrophoretic mobility of short DNA duplexes, *Nucl. Acids Res.* **16**, 6803 (1988).
 - ⁶⁸ J. Wang, P. Cieplak, and P. A. Kollman, How well does a restrained electrostatic potential (RESP) model perform in calculating conformational energies of organic and biological molecules, *J. Comp. Chem.* **21**, 1049 (2000).
 - ⁶⁹ L. McFail-Isom, C. C. Sines, and L. D. Williams, DNA structure: Cations in charge?, *Curr. Opin. Struct. Biol.* **9**, 298 (1999).
 - ⁷⁰ K. J. McConnell and D. L. Beveridge, DNA structure: What's in charge?, *J. Mol. Biol.* **304**, 803 (2000).
 - ⁷¹ A. D. Mirzabekov and A. Rich, Asymmetric lateral distribution of unshielded phosphate groups in nucleosomal DNA and its role in DNA bending, *Proc. Natl. Acad. Sci. USA* **76**, 1118 (1979).
 - ⁷² J. K. Strauss and L. J. Maher, III, DNA bending by asymmetric phosphate neutralization, *Science* **266**, 1829 (1994).
 - ⁷³ M. A. Young, B. Jayaram, and D. L. Beveridge, Intrusion of counterions into the spine of hydration in the minor groove of B-DNA: Fractional occupancy of electronegative pockets, *J. Am. Chem. Soc.* **119**, 59 (1997).
 - ⁷⁴ I. Rouzina and V. A. Bloomfield, DNA bending by small, mobile multivalent cations, *Biophys. J.* **74**, 3152 (1998).
 - ⁷⁵ H. R. Drew and A. A. Travers, DNA bending and its relation to nucleosome positioning, *J. Mol. Biol.* **186**, 773 (1985).
 - ⁷⁶ N. V. Hud and M. Polak, DNA-cation interactions: The major and minor grooves are flexible ionophores, *Curr. Opin. Struct. Biol.* **11**, 293 (2001).
 - ⁷⁷ T. E. Haran and D. M. Crothers, Cooperativity in A-tract structure and bending properties of composite TnAn blocks, *Biochemistry* **28**, 2763 (1989).
 - ⁷⁸ D. Hamelberg, L. D. Williams, and W. D. Wilson, Influence of the dynamic positions of cations on the structure of the DNA minor groove: Sequence-dependent effects, *J. Am. Chem. Soc.* **32**, 7745 (2001).
 - ⁷⁹ N. V. Hud and J. Feigon, Localization of divalent metal ions in the minor groove of DNA A-tracts, *J. Am. Chem. Soc.* **119**, 5756 (1997).
 - ⁸⁰ N. C. Stellwagen, S. Magnusdottir, C. Gelfi, and P. G. Righetti, Preferential counterion binding to A-tract DNA oligomers, *J. Mol. Biol.* **305**, 1025 (2001).
 - ⁸¹ R. Liebmann, *Lecture Notes in Physics* (Springer, Berlin, 1986), Vol. 251.
 - ⁸² R. E. Depew and J. C. Wang, Conformational fluctuations of DNA helix, *Proc. Natl. Acad. Sci. USA* **72**, 4275 (1975).
 - ⁸³ P. Anderson and W. Bauer, Supercoiling in closed circular DNA: Dependence upon ion type and concentration, *Biochemistry* **17**, 594 (1978).
 - ⁸⁴ C.-H. Lee, H. Mizusawa, and T. Kakefuda, Unwinding of double-stranded DNA helix by dehydration, *Proc. Natl. Acad. Sci. USA* **78**, 2838 (1981).
 - ⁸⁵ H. R. Drew and A. A. Travers, DNA structural variations in the E.coli tyrT promoter, *Cell* **37**, 491 (1984).
 - ⁸⁶ C. H. Laundon and J. D. Griffith, Curved helix segments can uniquely orient the topology of supertwisted DNA, *Cell* **52**, 545 (1988).
 - ⁸⁷ Y. Yang, T. P. Westcott, S. C. Pedersen, I. Tobias, and W. K. Olson, Effects of localized bending on DNA supercoiling, *Trends Biochem. Sci.* **20**, 313 (1995).
 - ⁸⁸ R. E. Dickerson, M. Bansal, C. R. Calladine, S. Diekmann, W. N. Hunter, O. Kennard, R. Lavery, H. C. M. Nelson, W. K. Olson, W. Saenger, Z. Shakked, H. Sklenar, D. M. Soumpasis, C.-S. Tung, E. von Kitzing, A. H.-J. Wang, and V. B. Zhurkin, Definitions and nomenclature of nucleic acid structure parameters, *J. Mol. Biol.* **205**, 787 (1989).
 - ⁸⁹ A. K. Mazur, Internal correlations in minor groove profiles of experimental and computed B-DNA conformations, *J. Mol. Biol.* **290**, 373 (1999).